



# Protective effect of ascorbic acid against double-strand breaks in giant DNA: Marked differences among the damage induced by photo-irradiation, gamma-rays and ultrasound



Yue Ma<sup>a</sup>, Naoki Ogawa<sup>a</sup>, Yuko Yoshikawa<sup>b</sup>, Toshiaki Mori<sup>c</sup>, Tadayuki Imanaka<sup>b</sup>, Yoshiaki Watanabe<sup>a</sup>, Kenichi Yoshikawa<sup>a,\*</sup>

<sup>a</sup> Faculty of Biological and Medical Sciences, Doshisha University, Kyotanabe 610-0394, Japan

<sup>b</sup> Research Organization of Science and Technology, Ritsumeikan University, Kusatsu 525-8577, Japan

<sup>c</sup> Radiation Research Laboratory, Osaka Prefecture University, Sakai 599-8570, Japan

## ARTICLE INFO

### Article history:

Received 18 July 2015

In final form 21 August 2015

Available online 28 August 2015

## ABSTRACT

The protective effect of ascorbic acid against double-strand breaks in DNA was evaluated by single-molecule observation of giant DNA (T4 DNA; 166 kbp) through fluorescence microscopy. Samples were exposed to three different forms of radiation: visible light,  $\gamma$ -ray and ultrasound. With regard to irradiation with visible light, 1 mM AA reduced the damage down to ca. 30%. Same concentration of AA decreased the damage done by  $\gamma$ -ray to ca. 70%. However, AA had almost no protective effect against the damage caused by ultrasound. This significant difference is discussed in relation to the physico-chemical mechanism of double-strand breaks depending on the radiation source.

© 2015 The Authors. Published by Elsevier B.V. This is an open access article under the CC BY license (<http://creativecommons.org/licenses/by/4.0/>).

## 1. Introduction

DNA plays an essential role in the development and function of all known living organisms, since it encodes the genetic instructions. Therefore, damage to DNA is a major problem for living things. DNA damage is currently categorized into 4 types: base changes, cross-linking, and single- and double-strand breaks (DSBs). Among these, DSBs are considered to be the most serious because they lead to cancer and cell death [1–6]. Many studies have been performed to detect DSBs both in vivo and in vitro. The polymerase chain reaction can be used to detect DNA damage through observation of the termination of amplification [7,8]. Immunological assays are also commonly used for the detection of oxidative DNA damage through the use of an antibody or immunoglobulin [7,9]. In situ hybridization provides information on specific changes in certain DNA sequences [7,10]. A comet assay can detect double-strand breaks in DNA, although a quantitative evaluation is almost impossible [7,11]. Despite the availability of these methods, it has been difficult to estimate the number of double-strand breaks in a reliable manner, especially for genome-sized long DNA molecules. Recently, it has been demonstrated that the direct visualization of single giant DNA molecules by the use of fluorescence

microscopy provide useful information on the structure and function of genomic DNA molecules [12–14], including the application to analyze DSBs in a quantitative manner [15–23].

Reactive oxygen species (ROS), which are generated through various processes, have been considered to be a major contributing factor to DNA strand breaks. The use of an antioxidant is an efficient method for protecting DNA from damage induced by reactive oxygen radicals [1,24]. Ascorbic acid (AA), or vitamin C, is a representative antioxidant. Pauling claimed that AA could play a significant role in maintaining good health in humans [25,26]. It has been reported that AA can reduce ROS in human sperm cells to minimize the risk of DNA damage [27]. In the present study, to evaluate the protective effects of AA on genome DNA molecules in a quantitative manner, we measured DSBs caused by photo-irradiation in the presence of sensitizer,  $\gamma$ -rays and ultrasound through single-molecule observation by fluorescence microscopy. To observe the effect of photo-induced reaction oxygen species, we used YOYO-1, quinolinium, 1,1'-[1,3-propanediyl-bis [(dimethylimino)-3,1-propanediyl]] bis [4-[(3-methyl-2(3H)-benzoxazolylidene)-methyl]-tetraiodide, as a photosensitizer to generate reactive oxygen, and performed the real-time observation of double-strand breaks in individual DNA molecules, where YOYO-1 also helps to visualize DNA as a fluorescence dye [17]. With regard to  $\gamma$ -ray and ultrasound, the numbers of DSBs were evaluated in terms of the average length of DNA molecules at different degrees of irradiation in the presence of AA.

\* Corresponding author.

E-mail address: [keyoshik@mail.doshisha.ac.jp](mailto:keyoshik@mail.doshisha.ac.jp) (K. Yoshikawa).

## 2. Materials and methods

### 2.1. Materials

T4 phage DNA (166 kbp, contour length 57  $\mu\text{m}$ ) was purchased from Nippon Gene (Toyama, Japan). A fluorescent cyanine dye, YOYO-1 (quinolinium, 1,1'-[1,3-propanediyl-bis[(dimethylimino)-3,1-propanediyl]] bis [4-[(3-methyl-2(3H)-benzoxazolylidene)-methyl]]-tetraiodide), was purchased from Molecular Probes, Inc. (Oregon, USA). Antioxidants, 2-mercaptoethanol (2-ME) and AA, and other necessary chemicals were purchased from Wako Pure Chemical Industries (Osaka, Japan).

### 2.2. Real-time observation of photo-induced breakage

In fluorescence microscopic observations, to minimize intermolecular aggregation, measurements were conducted at a low DNA concentration (0.1  $\mu\text{M}$  in nucleotide units). T4 phage DNA was dissolved in buffer solution with YOYO-1 in 10 mM Tris-HCl (pH: 7.5). To evaluate the protective effects against double-strand breaks, AA was added to samples with final concentrations of 0.5 mM and 1.0 mM. 2-ME (concentration: 4% (v/v)) was added to the samples to slow the photo-cleavage reaction to a level that was suitable for real-time observation.

The double-strand damage in individual DNA molecules was observed at a peak emission wavelength of 510 nm under strong light illumination. Fluorescence DNA images were captured by use of an Axiovert 135 TV microscope (Carl Zeiss, Oberkochen, Germany) equipped with an oil-immersed 100 $\times$  objective lens, and recorded on DVD through an EBCCD camera (Hamamatsu Photonics, Hamamatsu, Japan). The recorded videos were analyzed by VirtualDub, a free and open-source video-capture and video-processing utility for Microsoft Windows written by Avery Lee. All observations were carried out at around 20  $^{\circ}\text{C}$  [16,17].

### 2.3. Gamma-ray and ultrasound irradiation

T4 phage DNA (final concentration: 0.1  $\mu\text{M}$ ) was dissolved in Tris-HCl (concentration: 10 mM) buffer solution at pH 7.5. After AA was added to the DNA solution at either 0.5 mM or 1.0 mM, the samples were irradiated by  $^{60}\text{Co}$   $\gamma$ -ray at a dose rate of 3860 Gy/h. The quantity of  $\gamma$ -rays was controlled by the duration of irradiation [17,21].

Ultrasound for irradiation was provided by two Langevin transducers (FBL28452HS; FUJI CERAMICS, Fujinomiya, Japan) and the power was controlled by adjusting the transducers. The solutions for irradiation contained 0.1  $\mu\text{M}$  T4 in the presence and absence of 0.1  $\mu\text{M}$  AA (final concentration: 1.0 mM) with 10 mM Tris-HCl buffer [18].

### 2.4. Measurement of the length of single DNA molecules by fluorescence microscopy

DNA molecules were fixed on a glass surface after the addition of YOYO-1 (final concentration: 1  $\mu\text{M}$ ). Glasses were pre-treated with poly-(L-lysine) (concentration: 0.05% (v/v)) solution, and washed repeatedly with distilled water. A droplet (15  $\mu\text{l}$ ) of a sample was adsorbed on a modified glass slide and covered with a glass coverslip under weak shear. Fluorescence images were observed with an Axiovert 135 TV microscope (Carl Zeiss, Oberkochen, Germany) and analyzed by free software, ImageJ (National Institute of Mental Health, MD, USA) [17,18].

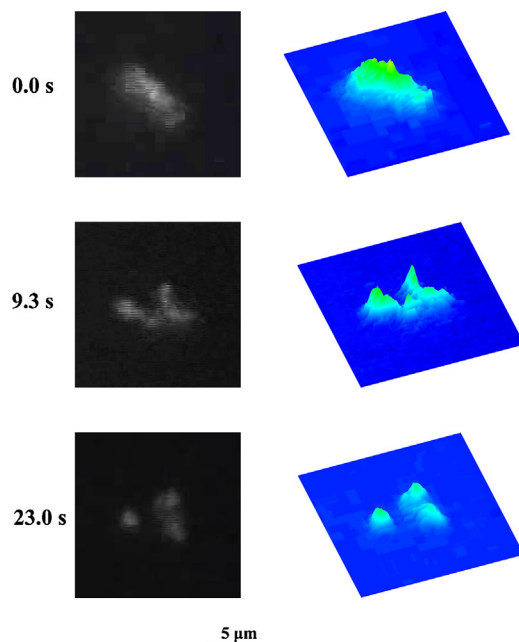


**Figure 1.** Example of the real-time observation of double-strand breaks. Fluorescence microscopic images on single T4 DNA molecule under photo-irradiation (left) and the corresponding quasi-three-dimensional profiles of the fluorescence-intensity distribution (right). (Fluorescent dye YOYO-1: 0.05  $\mu\text{M}$ , ascorbic acid: 1.0 mM.)

## 3. Results and analysis

### 3.1. Protective effect of ascorbic acid against photo-induced DNA double-strand breaks

Figure 1 exemplifies the real-time observation of double-strand breaks and the corresponding quasi-three-dimensional profiles of the fluorescence-intensity distribution for a DNA molecule. From the visual confirmation of breakage, the breakage time,  $\tau$ , was evaluated by taking time zero as the moment when focused illumination was initiated. The average breakage time,  $\langle\tau\rangle$ , was calculated from the data for 40–50 DNA molecules. In the absence of AA,  $\langle\tau\rangle$  was 13 s.  $\langle\tau\rangle$  increased with the addition of AA:  $\langle\tau\rangle$  was 22 and 26 s in the presence of 0.5 and 1.0 mM AA, respectively. Figure 2a shows the time-dependent increase on the percentage of damaged DNA molecules under of the double-strand breaks under photo-irradiation. In order to gain further insight on the mechanism of the double-strand breaks, as in Figure 2b we rescaled the graph by placing the logarithm of the probability  $P$  of surviving DNA and the square of the duration of irradiation on the vertical and horizontal axes, respectively. The linear relationships in the figure implies that the kinetics is given as the multiplication of two independent events, i.e., the double-strand breaks are induced as a two-step mechanism as the result of occurrence of two single-strand breaks nearby each other on the both sides of double-stranded helix [16,17]. As illustrated in Figure 3a, in the two-step mechanism, single-strand breaks, or nicks, are generated randomly along double-strand DNA molecules under irradiation (Step 1). When another single-strand break occurs on the other DNA strand near a certain nick, a double-strand break (Step 2) is generated, which is recognized as fragmentation in the single-molecule measurement (Figure 1). A DNA chain is cut into fragments only when the sugar phosphate backbones on both sides are broken. We have previously reported the details of the kinetics of DSBs through such a two-step mechanism [16,17]. In the following discussion, we

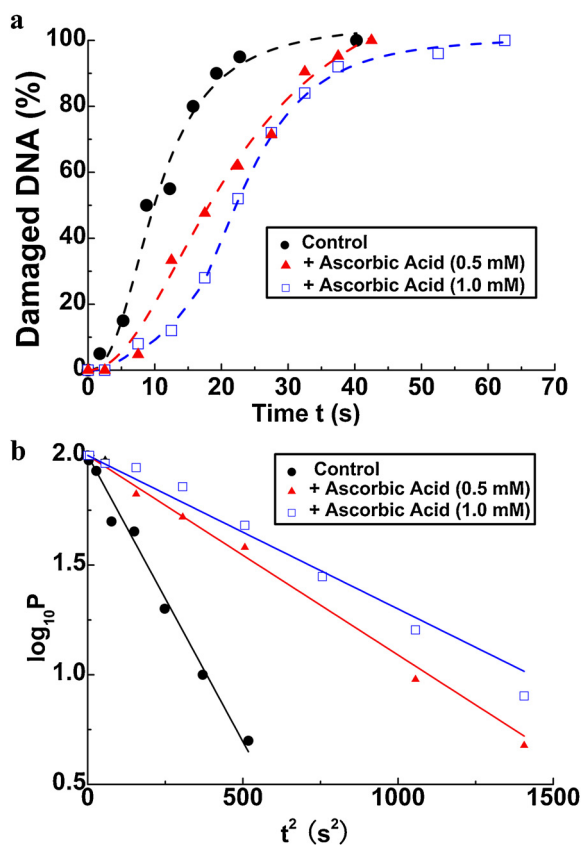


**Figure 2.** Photo-induced DSBs. (a) Time-dependence of the percentage of damaged DNA molecules. (b) Relationship between  $t^2$  and  $\log_{10} P$ . ( $P$  is the percentage of surviving DNA molecules under photo-irradiation, which was calculated as  $[100\% - (\text{percentage of damaged DNA})]$ .)

only describe the essence on the theoretical scheme to analyze the experimental data.

Under constant illumination with a power of  $I$ , the number of nicks along a single DNA molecule will increase as in Eq. (1), where  $\alpha$  is a constant:

$$dn/dt = \alpha I \quad (1)$$

By denoting  $P$  as the probability of surviving DNA molecules against double-strand damage, the rate of the decrease in  $P$  can be represented as the product of  $n$  (number of nicks) and  $P$ :

$$dP/dt = -knP = -k\alpha ItP \quad (2)$$

where  $k$  is a rate constant. Then, we obtain

$$\log_{10}(P/P_0) \propto -\alpha It^2 \quad (3)$$

By considering the initial condition as  $P_0 = 1$  at  $t = 0$ , we obtain Eq. (4):

$$\log_{10}(P) = -K^V t^2 \quad (4)$$

where  $K^V$  is a rescaled kinetic constant. Thus, the slopes in Figure 2b provide quantitative information on the protective effect of AA against photo-induced double-strand breaks.

The linear relationships in Figure 2b actually demonstrate the validity of Eq. (4) for photo-induced DSBs, and from such relationships we can evaluate the relative kinetic constant  $K^V/K_0^V$ , where  $A_0$  is the case without AA. The difference in the slopes in Figure 2b indicate that the kinetics on the double-strand breaks in the presence of 0.5 mM and 1.0 mM AA are about 40% and 30%, respectively, of those in the absence of AA. It is also to be noted that such protective effect

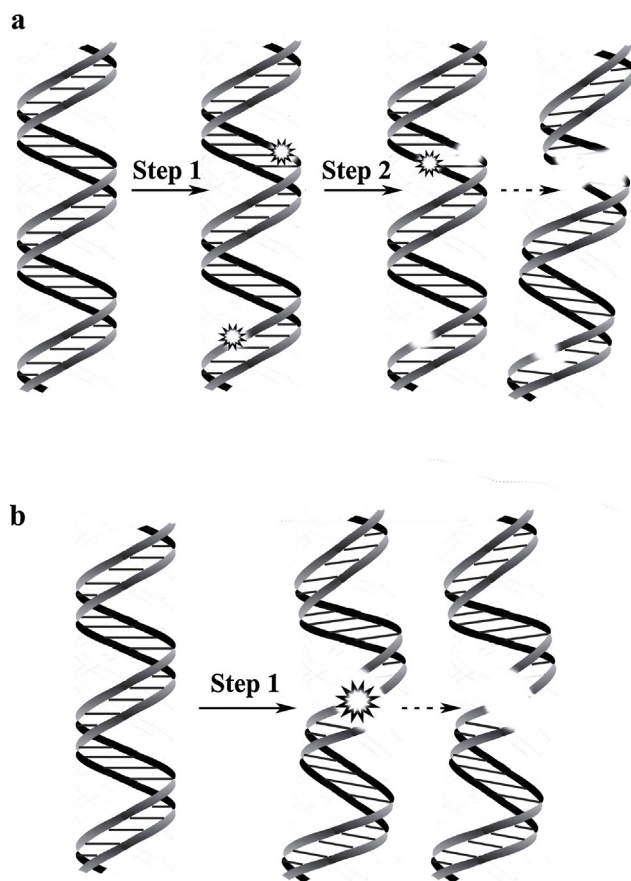


**Figure 3.** Schematic illustrations of a double-strand break. (a) Two-step mechanism. (b) One-step mechanism.

of AA is expected to work for the kinetics of single-strand breaks, as suggested from the above mentioned theoretical framework.

### 3.2. Protective effect of ascorbic acid against gamma-ray-induced DNA double-strand breaks

Fluorescence images of DNA fixed on a glass substrate for specimens after  $\gamma$ -ray radiation are exemplified in Figure 4a. As shown, the length of DNA molecules decreases with an increase in the intensity of  $\gamma$ -ray irradiation for both with and without AA. The average control length of DNA,  $\langle L_0 \rangle$ , was determined to be 20.3  $\mu\text{m}$  for the samples without  $\gamma$ -ray radiation. This is somewhat smaller than the natural contour length (57  $\mu\text{m}$ ) and can be attributed to the procedure used to extract and purify T4 DNA molecules from the phage. Figure 4b shows the change in the average length  $\langle L \rangle$  of DNA as a function of the irradiation dose. If the average number of DSBs per individual DNA molecule is defined as  $\langle n \rangle$ , the following relationship is derived under the assumption of a one-step mechanism (Figure 2b) [16,17]:

$$\langle n \rangle \approx \langle L_0 \rangle / \langle L \rangle - 1 \quad (5)$$

The proportionality of  $\langle n \rangle$  with respect to the irradiation dose with  $\gamma$ -ray is shown in Figure 4c. Thus, we assumed Eq. (6) by introducing a kinetic constant  $K^V$ :

$$n = K^V D \quad (6)$$

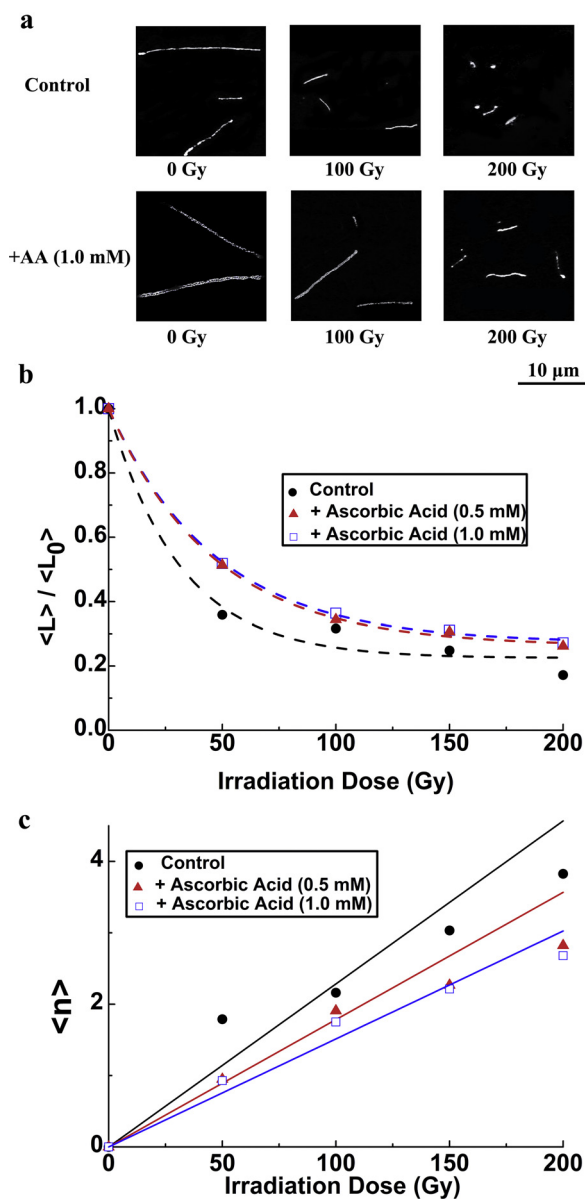


**Figure 4.**  $\gamma$ -Ray-induced DSBs. (a) Fluorescence microscopic images of DNA molecules fixed on a glass surface after irradiation with different doses of  $\gamma$ -rays. (b) Average lengths of DNA,  $\langle L \rangle$ , vs. the irradiation dose of  $\gamma$ -rays. (c) Number of DSBs per DNA molecule, vs. the irradiation dose of  $\gamma$ -rays.

### 3.3. Protective effect of ascorbic acid against ultrasound-induced DNA double-strand breaks

Figure 5a exemplifies the DNA observations after exposure to ultrasound. We analyzed the experimental data in the same manner as for  $\gamma$ -ray-induced double-strand breaks. Based on the data on the sound pressure level-dependence of the average length ( $L$ ) given in Figure 5b, we obtained a graph of the average number of breaks per original DNA molecule,  $\langle n \rangle$ , with respect to the sound pressure, as shown in Figure 5c. This confirms the existence of a threshold value of sound pressure for DNA double-strand breaks; below this threshold, the probability of double-strand breaks is essentially zero [18]. Above the threshold,  $\langle n \rangle$  increases linearly with the sound pressure. Interestingly, the nature of the increase in  $\langle n \rangle$  is almost the same independent of the presence or absence of AA. These results demonstrate that AA does not have an obvious protective effect against ultrasound-induced DSBs.

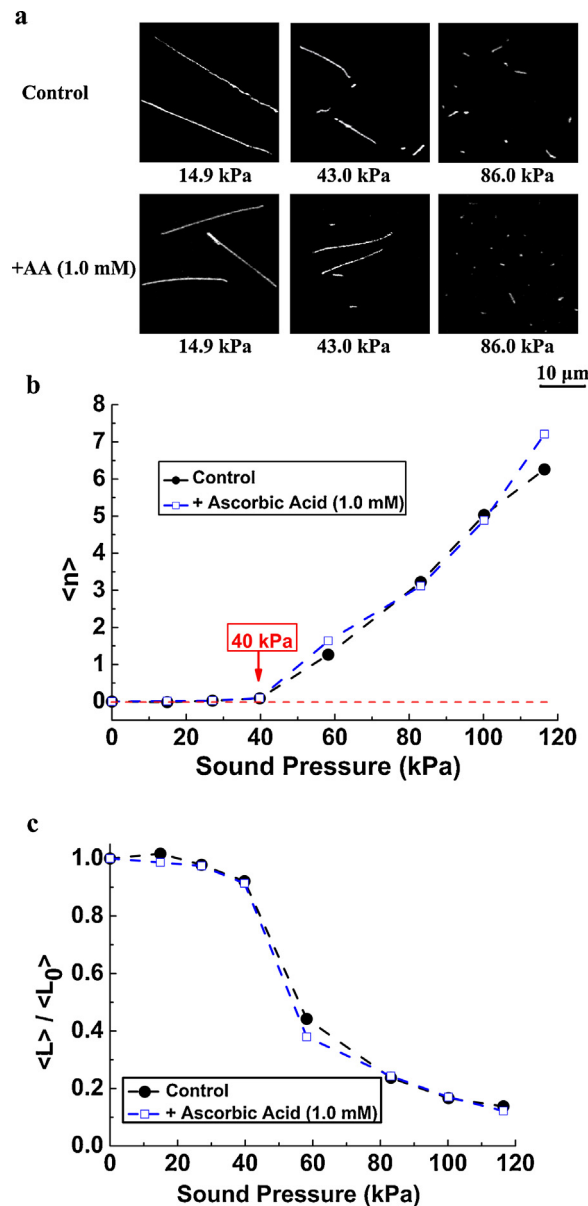


**Figure 5.** Ultrasound-induced DSBs. (a) Fluorescence microscopic images of DNA molecules fixed on a glass surface after exposure to ultrasound at different sound pressures. (b) Average lengths of DNA,  $\langle L \rangle$ , vs. the sound pressure of ultrasound. (c) Number of DNA double-strand breaks per molecule,  $\langle n \rangle$ , vs. the sound pressure of ultrasound.

As in the analysis of  $\gamma$ -ray-induced DSBs, the slope from the linear relationship with the intercept of horizontal axis at the threshold sound pressure  $p_0 = 40$  kPa, kinetic constant,  $K^U$ , is given as in Eq. (7):

$$n = K^U(p - 40) \quad (7)$$

where  $n$  is the number of DNA double-strand breaks and  $p$  (kPa) is the sound pressure of the ultrasound.

### 3.4. Comparison of the protective effects of ascorbic acid among photo-irradiation, gamma-rays and ultrasound

To compare the protective effects of AA against DSBs due to irradiation from different sources based on the experimentally available kinetic constants,  $K^V$ ,  $K^\gamma$  and  $K^U$ , we introduced a relative constant,  $K_1 = K/K_0$ , where  $K_0$  is the kinetic constant of the control group for each radiation source. Thus, it becomes possible

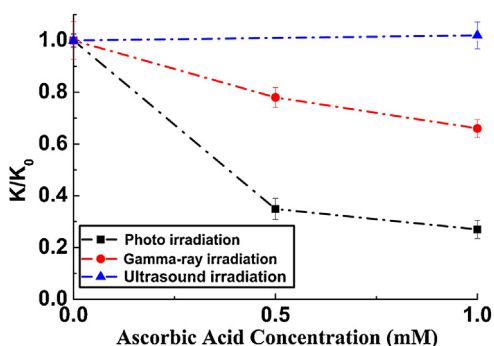


**Figure 6.** Difference in the protective effect of AA. Vertical axis is the relative kinetic constant  $K_1 = K/K_0$  on the reaction to cause DSBs at different concentrations of ascorbic acid, where  $K_0$  is the rate constant in the absence of AA. (For ultrasound-induced DNA damage, the kinetic constants are adapted from the threshold sound pressure, whereas the data are essentially the same for the kinetic parameters provided from the slopes, as shown in Figure 5c.)

to compare the degree of protective effect by AA, regardless the mechanism of the DSBs, either one-step or two-step. Changes in the relative constant  $K_1$  under different concentrations of AA are shown in Figure 6.

AA decreased the DNA damage caused by the exposure to visible light and this protective effect was enhanced with an increase in the concentration of AA. The DSBs induced by visible light decreased by about 65% in 1.0 mM AA solution. Although AA had a similar protective effect against  $\gamma$ -ray-induced DSBs, the damage was reduced by only around 30% in 1.0 mM AA solution, which is not as good as the protective effect against photo-induced damage. On the other hand, AA did not have any obvious protective effect against DSBs caused by ultrasound, where the kinetic constant is essentially the same as that in the absence of AA.

#### 4. Discussion

The protective effects of ascorbic acid against double-strand breaks in giant DNA molecules, which were caused by photo-irradiation in the presence of sensitizer,  $\gamma$ -rays and ultrasound, were tested at the level of single DNA molecules.

With regard to photo-induced DSBs, AA obviously reduced the number of breaks and this inhibitory effect increased with an increase in the AA. As for the DNA damage caused by  $\gamma$ -rays, the protective effect of AA is somewhat weaker compared to the case of photo-induced damage. On the contrary, for the damage by ultrasound, AA did not show any obvious protective effects against DSBs.

Previous studies have shown that there are two main mechanisms for the development of radiation-induced DSBs [16,17]. For  $\gamma$ -ray radiation, single step is the main process to cause DSBs (see Figure 3b), which is attributed to the generation of number of ROS upon the incident of individual photon of  $\gamma$ -ray. Whereas photo-radiation causes DSBs through two step mechanism (Figure 3a)

by reflecting that each single photon causes mostly single ROS and thus induces only single strand break. Then, when a second single strand break occurs where near the existing single strand break, DSB is caused, i.e., the two step mechanism. Summarizing the results and discussion we may conclude as that: (1) The significant protective effect of AA against photo-induced damage may reflect the effective diminish of ROS by AA. (2) For the  $\gamma$ -ray induced DSB, the protective effect by AA is a little bit weaker than the case of photo irradiation. This may be due to the generation of numbers of ROS by single photon of  $\gamma$ -ray. Surviving oxygen species against the diminishment effect by AA may cause DSBs. (3) As for the DSBs by ultrasound, damage is caused by the shockwave through the generation of cavitations [18]. Thus, the chemical effect of AA to diminish ROS is considered to be negligibly small for the protection of DSBs.

#### Acknowledgement

This work was partly supported by Kakenhi (Nos. 15H02121, 25103012 and 25390038).

#### References

- [1] S. Loft, H.E. Poulsen, *J. Mol. Med.* 74 (1996) 297.
- [2] T. Weinert, *Cell* 94 (1998) 555.
- [3] M. Fenech, *Ann. N.Y. Acad. Sci.* 854 (1998) 23.
- [4] T. Rich, R.L. Allen, A.H. Wyllie, *Nature* 407 (2000) 777.
- [5] J. Bradbury, S. Jackson, *Biochem. Soc. Trans.* 31 (2003) 40.
- [6] J.H. Hoeijmakers, *N. Engl. J. Med.* 361 (2009) 1475.
- [7] S. Kumari, R.P. Rastogi, K.L. Singh, S.P. Singh, R.P. Sinha, *EXCLI J.* 7 (2008) 44.
- [8] G. Schochetman, C.-Y. Ou, W.K. Jones, *J. Infect. Dis.* (1988) 1154.
- [9] A.M. Amaro, K.B. Hallberg, E.B. Lindström, C.A. Jerez, *Appl. Environ. Microbiol.* 60 (1994) 3470.
- [10] G.I. McFadden, *Methods Cell Biol.* 49 (1995) 165.
- [11] W. Liao, M.A. McNutt, W.-G. Zhu, *Methods* 48 (2009) 46.
- [12] A. Estévez-Torres, D. Baigl, *Soft Matter* 7 (2011) 6746.
- [13] D. Lundberg, N.V. Berezhnoy, C. Lu, N. Korolev, C.-J. Su, et al., *Langmuir* 26 (2010) 12488.
- [14] A.A. Zinchenko, *Polym. Sci. Ser. C* 54 (2012) 80.
- [15] H. Kurita, T. Takata, H. Yasuda, K. Takashima, A. Mizuno, *Chem. Phys. Lett.* 493 (2010) 165.
- [16] Y. Yoshikawa, M. Suzuki, N. Yamada, K. Yoshikawa, *FEBS Lett.* 566 (2004) 39.
- [17] Y. Yoshikawa, T. Mori, M. Suzuki, T. Imanaka, K. Yoshikawa, *Chem. Phys. Lett.* 501 (2010) 146.
- [18] K. Yoshida, N. Ogawa, Y. Kagawa, H. Tabata, Y. Watanabe, et al., *Appl. Phys. Lett.* 103 (2013) 063705.
- [19] S.F. Shimobayashi, T. Iwaki, T. Mori, K. Yoshikawa, *J. Chem. Phys.* 138 (2013) 174907.
- [20] Y. Yoshikawa, M. Suzuki, N. Chen, A.A. Zinchenko, S. Murata, et al., *Eur. J. Biochem.* 270 (2003) 3101.
- [21] M. Suzuki, C. Crozatier, K. Yoshikawa, T. Mori, Y. Yoshikawa, *Chem. Phys. Lett.* 480 (2009) 113.
- [22] Y. Yoshikawa, N. Umezawa, Y. Imamura, T. Kanbe, N. Kato, et al., *Angew. Chem. Int. Ed.* 52 (2013) 3712.
- [23] T. Iwaki, T. Ishido, K. Hirano, A.A. Lazutin, V.V. Vasilevskaya, et al., *J. Chem. Phys.* 142 (2015) 145101.
- [24] A.P. Breen, J.A. Murphy, *Free Radic. Biol. Med.* 18 (1995) 1033.
- [25] L. Pauling, *Proc. Natl. Acad. Sci.* 67 (1970) 1643.
- [26] E. Cameron, L. Pauling, B. Leibovitz, *Cancer Res.* 39 (1979) 663.
- [27] C.G. Fraga, P.A. Motchnik, M.K. Shigenaga, H.J. Helbock, R.A. Jacob, et al., *Proc. Natl. Acad. Sci.* 88 (1991) 11003.